A&A 603, A120 (2017)
DOI: 10.1051/0004-6361/201730503

Astronomy & Astrophysics

Wolf-Rayet spin at low metallicity and its implication for black hole formation channels

Jorick S. Vink[1] and Tim J. Harries[2]

[1] Armagh Observatory and Planetarium, College Hill, Armagh BT61 9DG, Northern Ireland, UK
e-mail: jsv@arm.ac.uk
[2] Department of Physics and Astronomy, University of Exeter, Exeter EX4 4QL, UK

Received 26 January 2017 / Accepted 28 March 2017

ABSTRACT

Context. The spin of Wolf-Rayet (WR) stars at low metallicity (Z) is most relevant for our understanding of gravitational wave sources, such as GW 150914, and of the incidence of long-duration gamma-ray bursts (GRBs). Two scenarios have been suggested for both phenomena: one of them involves rapid rotation and quasi-chemical homogeneous evolution (CHE) and the other invokes classical evolution through mass loss in single and binary systems.
Aims. The stellar spin of WR stars might enable us to test these two scenarios. In order to obtain empirical constraints on black hole progenitor spin we infer wind asymmetries in all 12 known WR stars in the Small Magellanic Cloud (SMC) at $Z = 1/5\ Z_\odot$ and within a significantly enlarged sample of single and binary WR stars in the Large Magellanic Cloud (LMC at $Z = 1/2\ Z_\odot$), thereby tripling the sample of Vink from 2007. This brings the total LMC sample to 39, making it appropriate for comparison to the Galactic sample.
Methods. We measured WR wind asymmetries with VLT-FORS linear spectropolarimetry, a tool that is uniquely poised to perform such tasks in extragalactic environments.
Results. We report the detection of new line effects in the LMC WN star BAT99-43 and the WC star BAT99-70, along with the well-known WR LBV HD 5980 in the SMC, which might be undergoing a chemically homogeneous evolution. With the previous reported line effects in the late-type WNL (Ofpe/WN9) objects BAT99-22 and BAT99-33, this brings the total LMC WR sample to four, i.e. a frequency of ~10%. Perhaps surprisingly, the incidence of line effects amongst low Z WR stars is not found to be any higher than amongst the Galactic WR sample, challenging the rotationally induced CHE model.
Conclusions. As WR mass loss is likely Z-dependent, our Magellanic Cloud line-effect WR stars may maintain their surface rotation and fulfill the basic conditions for producing long GRBs, both via the classical post-red supergiant or luminous blue variable channel, or resulting from CHE due to physics specific to very massive stars.

Key words. stars: Wolf-Rayet – gravitational waves – stars: early-type – stars: evolution – techniques: polarimetric – stars: winds, outflows

1. Introduction

Long-duration gamma-ray bursts (GRBs) are amongst the brightest and most distant objects in the Universe (Tanvir et al. 2009; Cucchiara et al. 2011), implying that massive stars could live and die when the cosmos was just a few hundred million years old. The favoured progenitors are Wolf-Rayet (WR) stars at low metallicity (Woosley & Bloom 2006). In the collapsar scenario (MacFadyen & Woosley 1999) a rapidly rotating stellar core collapses into a black hole, thereby producing two narrow jets that are identifiable as a GRB. As of today the progenitors of GRBs are poorly constrained empirically, and one of the aims of our WR studies in low metallicity (Z) galaxies is to alleviate this shortcoming. The key physical sequence of events with respect to the GRB puzzle concerns the interplay between mass loss and rotation as a function of metallicity (Z), with the main idea that lower Z WR stars have weaker stellar winds than their galactic counterparts (Vink & de Koter 2005). This should lead to less spin-down of the progenitor WR star, enabling GRB conditions at low Z, for example via rotation-induced chemically homogeneous evolution (Yoon & Langer 2005; Woosley & Heger 2006).

A second major motivation for our study concerns the discovery of huge black hole masses in the merging event associated with GW150914, involving masses of order 30–40 $M_\odot$ (Abbott et al. 2016). This has led to a quest for constraints on the spin rates of black hole progenitors, i.e. WR stars. Given the huge masses inferred in the GW 150914 event, it is most likely that these extremely massive binary black holes were situated in a low-Z environment, as this is where the maximum black hole masses are predicted to be larger (Belczynski et al. 2010). It is therefore relevant to constrain the rotation rates of both single and binary WR stars in the low metallicity LMC ($Z = 1/2\ Z_\odot$) and SMC ($Z = 1/5\ Z_\odot$) galaxies.

The evolution of massive stars into WR stars and subsequently into black holes is still very uncertain, even for single star evolution. It is as yet not known whether internal magnetic fields couple the core to the envelope (e.g. Brott et al. 2011) or if massive stars rotate differentially (e.g. Georgy et al. 2013). For the former case, one may expect solid-body rotation, where the surface rotation rate inferred from observations may provide direct information on the spin properties of black hole progenitors. In the latter case, such inferences would be less direct, although relevant constraints on the core rotation of WR stars may still be obtained.

The special property of WR stars in comparison to canonical stars is that all their lines are in emission. This means that the traditional method involving the width of absorption lines

to measure the rotation rate (actually $v \sin i$) does not work for WR stars, but thanks to the line emission[1] an alternative tool is available to measure wind asymmetry resulting from rapid rotation. In its simplest form, the tool is based on the expectation that line photons arise over a larger volume than continuum photons, such that line photons undergo fewer scatterings and the emission-line flux is less polarized than the continuum when the wind geometry is aspherical when projected on the sky. This results in a smooth polarization variation across the line profile known as the line effect.

The high incidence of line effects amongst classical Be stars (Poeckert & Marlborough 1976) indicated that the envelopes of classical Be stars are not spherically symmetric. In a similar vein Harries et al. (1998) performed spectropolarimetry on a sample of 29 Galactic WR stars, finding that in the vast majority (of 80%) of WRs line effects were absent, indicating that the winds are spherical and rapid rotation is rare. Vink et al. (2011) and Gräfener et al. (2012) noted that the exceptions amongst the Galactic WRs were not randomly distributed but that there exists a highly significant correlation between line-effect WR stars and WRs with ejecta nebula. These authors argued that only the "young" WR stars, which have just recently transitioned from a previous red supergiant (RSG) or luminous blue variable (LBV) phase, rotate rapidly; this occurs presumably before strong Galactic WR winds during the rest of the WR phase ensure that the bulk of Galactic WR stars are spherical and rotating slowly. This suggests a post RSG or LBV "classical" scenario for the production of GRBs rather than quasi-chemical homogeneous evolution (CHE), as discussed in Vink et al. (2011) and Gräfener et al. (2012).

As WR winds in low metallicity environments are thought to be weaker (Vink & de Koter 2005; Gräfener & Hamann 2008; Hainich et al. 2015) one may possibly expect a higher incidence of line effect WR stars in the LMC and SMC. Vink (2007) therefore performed linear spectropolarimetry on a sample of the brightest 12 WRs in the LMC, discovering only 2 line effects in BAT99-22 and BAT99-33, which is similar to the incidence rate in the Galaxy. Here we extend our study to the even lower metallicity of the SMC and we also extend the LMC sample to a sample size that is comparable to that of the Galaxy. The sample of Vink (2007) was necessarily biased towards the brightest objects (with $V < 12$, mostly containing very late-type nitrogen-rich WR stars and/or binaries), and for an unbiased assessment one requires a larger sample. By encompassing the magnitude range $V < 14$, we triple the LMC sample (from 13 to 39).

Although both WN (nitrogen-rich) and WC (carbon-rich) stars might eventually become GRBs, WC stars are more likely to be the *direct* progenitors (e.g. Levan et al. 2016). Nevertheless, the physics of enhanced rotation is equally relevant for both sub-groups. Moreover, it is hard to tell whether WR stars in all mass ranges (and for all rotation rates and metallicities) always evolve from WN into WC stars (see e.g. Sander et al. 2012). For these reasons, we wish to constrain wind asymmetries and rotation rates amongst both sub-groups of WR stars. Furthermore, we wish to correlate linear polarization and rapid rotation with binarity. The larger data set enables us to correlate linear polarization with binarity, as radial velocity (RV) surveys for binary WRs in the LMC are available for both WC and WN stars, respectively (Bartzakos et al. 2001; Foellmi et al. 2003), allowing us to address the question whether binarity is a prerequisite for observed linear polarization in WR stars.

[1] Shenar et al. (2014) have calculated the potential influence of rotation for WR emission line shapes.

The paper is organized as follows. In Sect. 2 we briefly describe the observations, data reduction, and analysis of the linear polarization data. This is followed by a description of the resulting line Stokes I and linear polarization profiles for the SMC and LMC WR stars in Sect. 3. In Sect. 4, we discuss the constraints these observations provide on WR spin rates and evolution, and GRB production models.

2. Observations, data reduction, and methodology

The SMC linear spectropolarimetry data were obtained during the nights of 2008 September 8, 9, and 10 during ESO Period 81 using the FORS spectrograph in PMOS mode. Apart from the grism, the data were obtained in a similar manner as for the brighter ($V < 12$) LMC sample of Vink (2007) during P78. Here we use the 300V grism and the GG375 order filter with a slit width of 2″, yielding a spectral resolution of approximately 20 Å. This spectral resolution is about three times lower than that of Vink (2007) for the LMC and Harries et al. (1998) for the Milky Way measurements.

The new LMC data were obtained in an almost identical way as our SMC data, during the nights of 2010 September 22–25 (ESO Period 85). Our LMC targets were selected from the fourth catalogue of Population I LMC WR stars by Breysacher, Azzopardi & Tester (1999; hereafter BAT) on the basis of their relative brightness ($V \lesssim 14$). Line-effect stars in the new LMC sample are seen down to V magnitudes of 14, suggesting that brightness is not a prerequisite for showing polarization. In order to obtain a sample as unbiased as possible, save for brightness, the objects were not selected on the basis of any known circumstellar (CS) geometries, spectral peculiarities, or binarity. The list of objects is given in Table 1 alongside their spectral types. Because the 26 new LMC objects are fainter than the 13 brighter LMC objects observed in cycle 78 by Vink (2007), we settle for lower spectral resolution, which should not pose any problems as WR stars have fast winds (of thousands km s^{-1}).

To analyse the linearly polarized component in the spectra, FORS was equipped with the appropriate polarization optics. Polarization and unpolarized standard stars were also observed. Data reduction consisted of the preparation of the images via the subtraction of a median bias frame and the construction of a median flat-field for each night. The flat-field was then normalized via a division with a smoothed copy and this normalized flat-field was subsequently divided into the target images. Wavelength calibrations were constructed using low-order polynomial fits to the dispersion curve defined by visually identified arc lines. The spectropolarimetric reduction then closely followed the method detailed by Harries & Howarth (1996), although no cross-talk correction was required since the ordinary (o) and extraordinary (e) spectra are well separated on the FORS images. The o and e spectra were first extracted and sky subtracted, wavelength calibrated, and rebinned onto a uniform wavelength array. The eight spectra (o and e spectra from the 0°, 45°, 22.5°, and 67.5°, images) were finally combined into Stokes I, Q, and U intensity spectra via the ratio method (e.g. Tinbergen 1996), formally propagating the shot-noise errors throughout to provide variances on Q and U.

Observations of an unpolarized standard (HD 10038) were taken during the LMC run and these indicated that the instrumental polarization was less than 0.1%. We also obtained spectra of polarized standard stars (NGC 2024, Hiltner 652, and BD-14 1922) and the polarization magnitudes of these objects showed good agreement with the literature values. However, the position angles (PAs) showed a small, consistent offset of 2°

Table 1. Polarization data of WR stars observed during the various VLT runs.

Name	Alt. names	Spec.Tp	V mag	$P^{\rm B}_{\rm cont}$ (%)	$\theta^{\rm B}_{\rm cont}$ (°)	$P^{\rm lit}$ (%)	$\theta^{\rm lit}$	Line effect	Binarity
SMC									
SMC-WR1	AV 2a	WN3	15.14	0.922 ± 0.03	41.0 ± 0.8				no
SMC-WR2	AV 39a	WN4.5	14.23	0.196 ± 0.02	154.0 ± 2.9				no
SMC-WR3	AV 60a	WN3	14.48	0.701 ± 0.02	131.0 ± 0.9				yes
SMC-WR4	AV 81, Sk 41	WN6p	13.35	0.416 ± 0.02	126.0 ± 1.3				no
SMC-WR5	HD 5980	WN5	11.08	0.117 ± 0.02	27.6 ± 4.7			x	yes
SMC-WR6	AV 332, Sk 108	WN3	12.30	0.416 ± 0.01	122.2 ± 0.8				yes
SMC-WR7	AV 336a	WN2	12.93	0.263 ± 0.02	119.7 ± 1.8				yes
SMC-WR8	Sk 188	WO4	12.81	0.221 ± 0.02	103.2 ± 2.2				yes
SMC-WR9		WN3	15.23	0.437 ± 0.03	132.0 ± 1.6				?
SMC-WR10		WN3	15.76	0.458 ± 0.03	167.5 ± 2.0				no
SMC-WR11		WN3	14.97	0.408 ± 0.03	139.2 ± 2.4				no
SMC-WR12	SMC-054730	WN3	15.46	0.922 ± 0.03	41.0 ± 0.8				no
LMC BAT99									
7		WN4b	14.10	0.888 ± 0.022	34.3 ± 0.7				no
8		WC4	14.08	0.789 ± 0.029	34.5 ± 1.0				no?
9		WC4	14.05	1.164 ± 0.045	31.9 ± 1.1				no?
10	R 64	WC4+O9.5	13.61	0.417 ± 0.011	66.1 ± 0.7	0.66 ± 0.09	76 ± 4		no
11		WC4	13.01	0.413 ± 0.043	23.6 ± 3.0				no
14		WN4o+OB	13.7	0.651 ± 0.026	30.6 ± 1.1				no
19		WN4b+O5	13.76	0.052 ± 0.020	3.3 ±11.0				yes
20		WC4+O	14.01	2.322 ± 0.031	178.3 ± 0.4				no
21		WN4o+OB	13.11	0.632 ± 0.015	32.3 ± 0.7				no
34		WC4+OB	12.72	0.404 ± 0.020	31.5 ± 1.4				yes?
43		WN4o+OB	14.18	0.611 ± 0.019	10.1 ± 0.9			x	yes
47		WN3b	14.11	0.516 ± 0.033	28.0 ± 1.9				no
52		WC4	13.37	0.247 ± 0.030	30.2 ± 3.5				no
53		WC4+OB	13.17	0.565 ± 0.019	34.6 ± 1.0				yes?
59		WN4b+O8	13.33	0.188 ± 0.014	34.3 ± 2.2	0.17 ± 0.27	111± 29		?
61		WC4	13.04	0.301 ± 0.025	35.0 ± 2.3	0.27 ± 0.10	31 ± 11		no
64		WN4o+O9	14.39	0.538 ± 0.018	49.7 ± 1.0				yes
67		WN5ha	13.89	1.256 ± 0.024	36.2 ± 0.6				no
70	Sk -69 207	WC4+OB	13.79	2.205 ± 0.045	0.0 ± 0.6	0.95 ± 0.13	19 ± 4	x	no
84		WC4+OB	13.00	0.399 ± 0.020	164.1 ± 1.4	0.91 ± 0.20	171± 7		no
92	R 130	WN6+B1	11.51	0.943 ± 0.011	87.9 ± 0.3				
117	R 146	WN5ha	12.99	1.025 ± 0.021	38.5 ± 0.6	0.70 ± 0.26	48 ± 10		no
122	R 147	WN5(h)	13.06	1.487 ± 0.020	32.3 ± 0.4	1.55 ± 0.18	31 ± 3		no
125		WC4+OB	13.18	1.164 ± 0.016	166.7 ± 0.4				yes?
126		WN4b+O8	13.35	0.932 ± 0.015	169.2 ± 0.5				?
127		WC5+O6	13.31	0.818 ± 0.014	163.6 ± 0.5				yes?
22	R 84	WN9h	12.09	0.235 ± 0.007	147.8 ± 0.9	0.30 ± 0.15	74 ±13	x	
27		WN5?b+B1Ia	11.31	0.254 ± 0.006	36.3 ± 0.7	0.22 ± 0.13	73 ± 15		no
28	R 90	WC6+O5-6V-III	12.23	1.038 ± 0.007	47.5 ± 0.2	0.77 ± 0.17	53 ± 6		yes
33	R 99	Ofpe/WN9	11.54	1.315 ± 0.007	106.2 ± 0.2			x	
38		WC4+O?	11.50	0.556 ± 0.007	21.1 ± 0.3	0.48 ± 0.15	16 ± 9		yes
39		WC4+O6V-III	12.51	0.445 ± 0.013	23.0 ± 0.9				yes
42	R 103	WN5?b+(B3I)	9.91	0.601 ± 0.007	24.5 ± 0.4		no		
55		WN11h	11.99	0.226 ± 0.009	30.7 ± 1.1				
85		WC4+OB	11.75	1.716 ± 0.007	104.1 ± 0.1	1.59 ± 0.09	99 ± 2		no
92	R 130	WN6+B1Ia	11.51	1.043 ± 0.006	81.6 ± 0.2				
107	R 139	WNL/Of	12.12	1.647 ± 0.006	70.1 ± 0.1				
118	R 144	WN6h	11.15	0.166 ± 0.006	20.6 ± 1.1	0.05 ± 0.14	48 ± 10		
119	R 145	WN6(h)	12.16	2.231 ± 0.006	81.2 ± 0.1	1.82 ± 0.23	79 ± 4		

Notes. The brighter 13 LMC stars from Vink (2007) are at the bottom. Names, spectral types, and V magnitudes (Cols. 1–4) are from Massey & Duffy (2001) and Massey et al. (2003) for the SMC, and from Breysacher et al. (1999, BAT99) for the LMC. The continuum polarization percentage and errors (over 4200–4600 Å) are in Col. 5. Systematic errors in the polarization are estimated to be of order 0.1%. PAs (θ) are listed in Col. 6. The literature values of the B-band PA and continuum polarization are from the catalogue of Mathewson & Ford (1970) (Cols. 7 and 8). Binary information is given in Col. 10, for the SMC from Shenar et al. (2016), and for the LMC from Bartzakos et al. (2001) for WCs and Foellmi et al. (2003) for WNs.

(relative to the literature values). More importantly, all spectra showed a slow PA fluctuation with wavelength. We found this PA rotation to be the same for all our polarized standards and it is attributable to a slight chromatism of the half-wave plate. We fitted this PA rotation with a 5th-order polynomial, under the pragmatic assumption that the PAs of the polarized standards are constant over the wavelength range of the data. We then used this polynomial fit to correct the polarization spectra of our targets.

The percentage linear polarization P and its position angle θ are determined in the following way:

$$P = \sqrt{(Q^2 + U^2)} \quad (1)$$

$$\theta = \frac{1}{2} \arctan\left(\frac{U}{Q}\right). \quad (2)$$

The achieved accuracy of the polarization data is in principle determined by photon-statistics only, however due to systematic effects the absolute accuracy might be lower. We do not correct for instrumental or interstellar polarization (ISP) as these are equal for line and continuum wavelengths. Depolarization line effects can be measured across the He II lines at 4686 Å, 6560 Å, and several other emission lines, such as the CIV line at 5805 Å for the WC stars. As WR stars have fast winds (of order thousands km s^{-1}), we easily resolve these lines for most targets[2].

A non-detection would imply the wind is circularly symmetric on the sky (to within the detection limit). The detection limit is inversely dependent on the signal-to-noise ratio (S/N) of the spectrum and the contrast of the emission line as the line emission is diluting or depolarizing the flux from the continuum. Following Davies et al. (2005), the detection limit for the maximum intrinsic polarization $\Delta P_{\rm limit}$ can be represented by

$$\Delta P_{\rm limit}(\%) = \frac{100}{SNR} \times \frac{l/c}{l/c - 1}, \quad (3)$$

where l/c refers to the line-to-continuum contrast.

Our final spectra had between 10^5 and 10^6 counts per spectral bin in the continuum, giving a polarization error of between ~0.3% and ~0.1% and the spectral resolution, measured from the arc spectra, was ~20 Å, corresponding to ~1000 km s^{-1}. In Figs. 1–4 we plot the calibrated polarization spectra of our targets binned to a constant error of 0.1% in polarization.

3. Results

The linear continuum polarization of hot stars is thought to be caused by scattering of stellar photons off electrons in the circumstellar environment, but in addition there may be an interstellar component to the measured level of polarization. The continuum (excluding the emission lines) polarization data for all our targets are summarized in Table 1 in the form of the mean B-band (4200–4600 Å) percentage polarization and its position angle θ (Cols. 5 and 6). Polarization variability is commonplace amongst hot massive stars (Hayes 1975; Lupie & Nordsieck 1987; St-Louis et al. 1987; Davies et al. 2005), and accordingly we do not seek perfect agreement between our continuum polarization measurements and those in earlier literature. In order to assess whether the data imply most of our targets are indeed intrinsically unpolarized, we compare our measured continuum polarization data to previous measurements (where available). Given that for most objects with previous polarization data available our PA values are consistent with earlier measurement, it is safe to assume that the measured polarization for the bulk of our targets is of interstellar origin, with possibly a small intrinsic polarization component in some cases (see below).

Plots of the spectropolarimetric data are presented in the different panels of Figs. 1–4. The polarization spectra are presented as triplots, consisting of Stokes I (lower panel), P (middle panel), and the PA θ (upper panel).

3.1. SMC objects

The line polarimetry data for the 12 SMC objects are shown in Fig. 1. We do not find any evidence for line effects in either the polarization percentage or the PA in our SMC data. Interestingly, for WR 5, which is the famous WR/LBV HD 5980, we have additional data available from our earlier P78 run (over a slightly different wavelength range). This P 78 data is plotted in Fig. 2. Here, firm line effects are detected across several of the strong He II emission lines.

Although at face value there appear to be line effects present in the triplot of WR 8, the PA excursions are not consistent with their Stokes I line emission wavelengths, and we therefore attribute these spikes to be anomalous and we do not consider WR 8 to be a line-effect star. We conclude that line effects are rare amongst SMC stars; we note that the line effect in HD 5980 might be special as this object has shown LBV type outbursts (Koeningsberger et al. 2010, and references therein), and that line effects amongst LBV might be more common than amongst WR stars (Davies et al. 2005).

3.2. LMC objects

The data for the 26 LMC WR stars are plotted in Figs. 3 and 4, and the continuum measurements are listed in Table 1. The earlier measurements on the brighter LMC stars from Vink (2007) are added at the bottom of the table. Regarding continuum measurements, a significant body of previous data is available in Mathewson & Ford (1970). Our PA and the previous PA agree within the error bars for BAT99-61, BAT99-84, BAT99-117, BAT-122, BAT99-28, BAT99-38, and BAT99-119. The agreement is still present for the remainder of the sample (within 2 or 3σ), except for R99-59 and BAT99-22, where the PA is seen to vary significantly. Perhaps these two objects are intrinsically polarized. However, whilst BAT99-22 does show a line effect (see below), BAT99-59 does not. Significant variations in the continuum PA might be interpreted as the result of wind clumping (Davies et al. 2005).

We next consider the polarization and PA in lines with respect to continuum levels. New line effects are detected in BAT99-43 and BAT99-70. Interestingly, as BAT99-43 is a WN star, whilst BAT99-70 is a WC star. So, it appears that line effects here are not confined to the WN spectral class. This situation is similar to that of the Milky Way, where a line effect was detected in the WC binary WR 137 (e.g. Harries et al. 1998), although the majority of detections were found amongst WN stars (Harries et al. 1998), coinciding with the presence of ejecta nebula (Vink et al. 2011).

[2] Some of the targets have slower winds and these line effects are thus unresolved. However, given that WR line effects are known to be consistent with simple depolarizations, rather than more subtle line polarization effects, e.g. Vink et al. (2002), we do not expect this to affect our results.

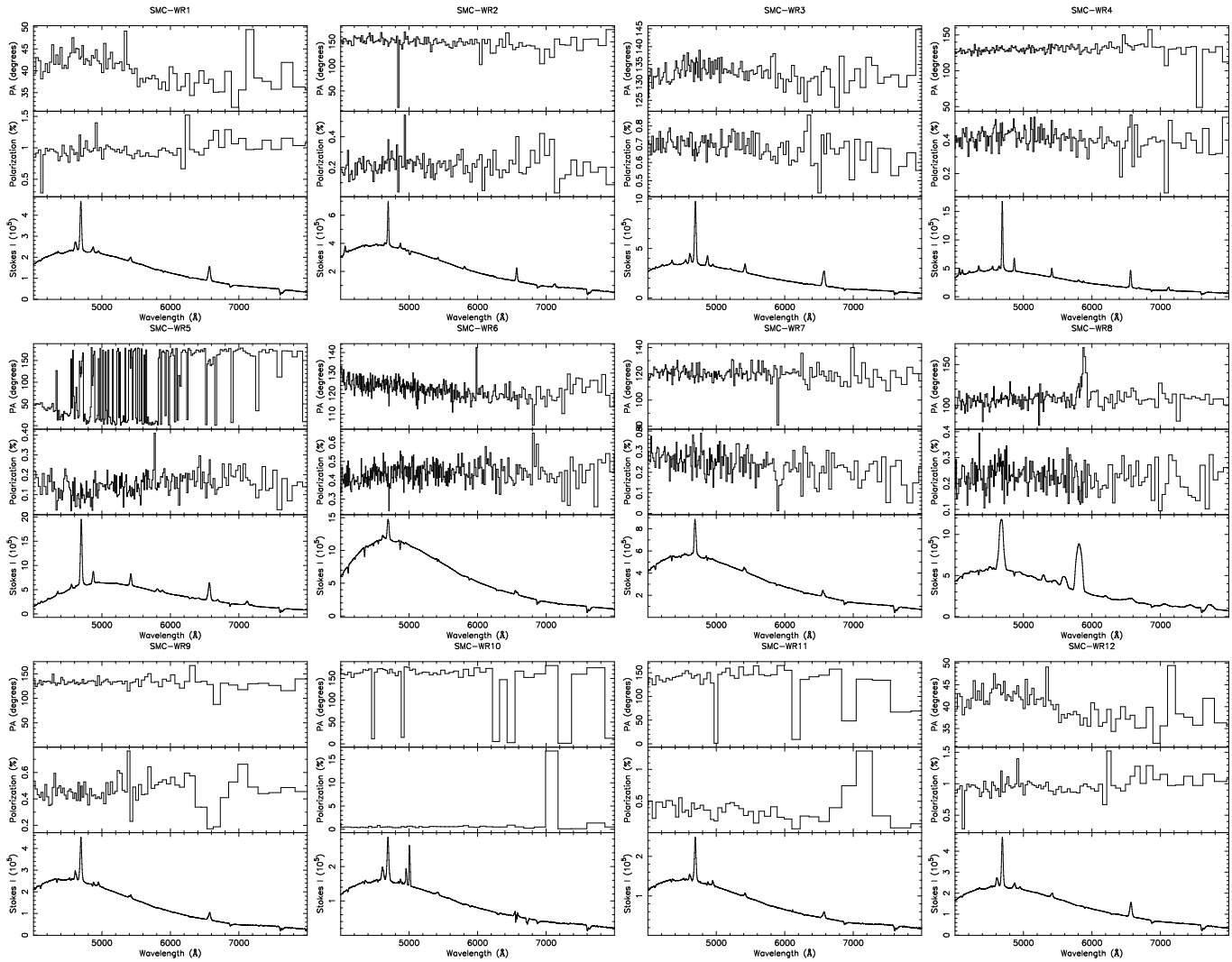

Fig. 1. Polarization spectra of the SMC WR objects. Stokes I spectra are shown in the *lowest panels of the triplots*, the levels of %Pol in *the middle panels*, whilst the PAs (θ; see Eq. (2)) are plotted in *the upper panels*. The data are rebinned such that the 1σ error in the polarization corresponds to 0.1% as calculated from photon statistics. In the *lowest panels*, the PA is sometimes seen to flip with wavelength by 90 degrees owing to small changes between QU quadrants when the observed polarization level is close to zero.

3.3. Binarity

One of the aims of our study is to find out whether binarity is a necessary condition for the detection of line effects in WR stars, as for instance the famous Galactic line-effect WC star WR 137 is a dust-producing binary. There are basically two distinct manners in which binarity might affect the detection of line effects.

The first way involves intra-binary scattering in close binaries (see e.g. the recent work by Hoffman & Lomax 2015, on V444 Cygni). The second way is more indirect with binary evolution possibly leading to more rapid rotation of the WR star (e.g. Cantiello et al. 2007), which may then result in a line effect in an identical way as would be the case for a rotating single WR star. Spectropolarimetric monitoring might be a useful tool to distinguish between these options.

We first wish to find out if binarity is a prerequisite for line effects amongst WR stars. For this reason, we correlate the incidence of line effects (Col. 9 in Table 1) with binarity (Col. 10). To first order, there is no notable correlation between the two, which may indicate that binarity is not required to create line effects. It is of course possible that single stars have had a binary past (e.g. de Mink et al. 2014; Justham et al. 2014), so we cannot exclude the possibility that binarity has played a role in the physics that causes the enhanced rotation. Nonetheless, the lack of correlation between line effects and binarity suggests that line effects in WR stars are not due to intra-binary scattering, thereby leaving stellar rotation as the most likely culprit.

It has been noted (St-Louis 2013) that many of the line-effect WR stars also exhibit co-rotating interaction regions (CIRs) and that perhaps it is these spiral variable structures that cause (or contribute to) the polarization rather than an axisymmetric flattened wind. Harries (2000) performed Monte Carlo radiative transfer computations of spiral structures and concluded this to be unlikely. Nevertheless, whether the line effects in WR stars are caused by flattened winds or CIRs (Ignace et al. 2009) in both cases one would link the line effects to stellar spin; i.e. line-effect stars are WR stars with enhanced stellar rotation (Harries et al. 1998).

4. Discussion

The incidence of line effects amongst LMC and SMC WR stars is low, which is unlikely to be due to their apparent faintness. Harries et al. (1998) noted that Galactic WR stars that show a

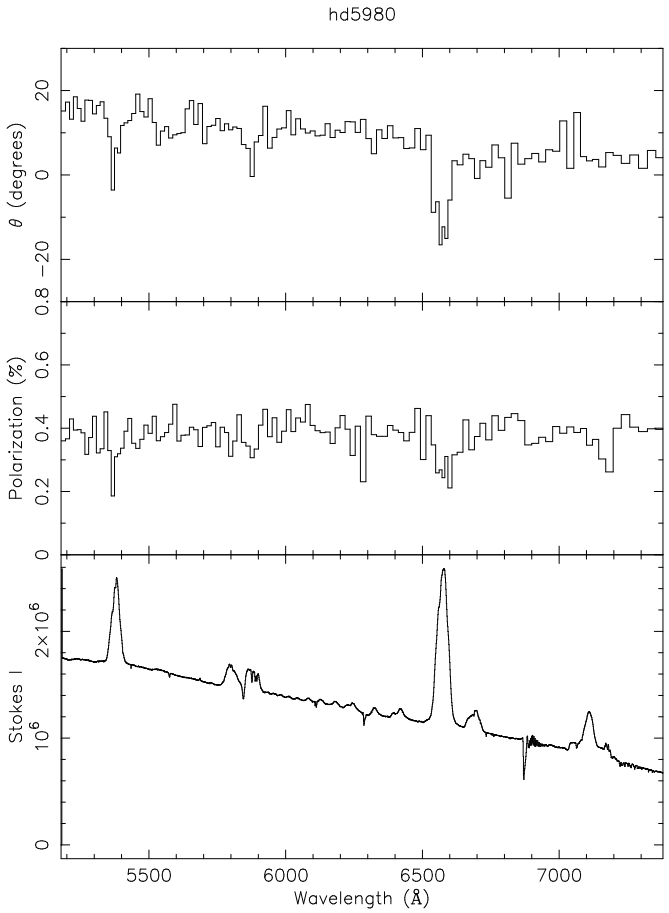

Fig. 2. Spectropolarimetric data for the WR/LBV star HD 5980 taken in 2006 during the P78 run. The plots are in the same format as Fig. 1.

line effect are polarized at levels >0.3%, arguing that polarized WRs are relatively rapid rotators. The S/N ratios achieved in the present study of MC WRs are large enough to detect similarly sized line effects.

Amongst the LMC WR sample, 2 out of 26, have line effects in addition to the 2 out of 13 from the brighter LMC Vink (2007) WR sample. This brings the overall incidence amongst the LMC sample to 4 out of 39, i.e. not significantly different from the 15–20% in the similarly sized Galactic sample (of 29) of Harries et al. (1998). Our SMC results of 1 in 12 comply as well. On the basis of the low incidence of line effects amongst the bright LMC sample Vink (2007) speculated his results could be explained if rapidly rotating WRs as progenitors for GRBs were confined to metallicities below that of the LMC (see also Wolf & Podsiadlowski 2007 on entirely different grounds). We can no longer draw this conclusion because the incidence of line-effect WR stars in the SMC, with a Z notably smaller than that of the LMC and Galaxy, is similarly low.

When we split the WR sample separately into WC stars, the frequency of Galactic WC stars of 1:8 does not increase either. In fact, for the LMC sample the frequency is 1:16. The lack of an increase in WR polarization at lower Z challenges the rotation-induced CHE model for GRB production.

4.1. Challenge to rotation-induced CHE for making GRBs

The most popular model for the production of GRBs is that of rotation-induced CHE (Yoon & Langer 2005; Woosley & Heger 2006; Levan et al. 2016). The attraction of the model is that rapid rotation mixes the star completely, which avoids the expansion of the star towards the red side of the HRD. The blueward evolution for the magnetic models (Brott et al. 2011), in combination with smaller WR mass loss at lower metal content (Vink & de Koter 2005), could ensure the maintenance of rapid rotation until collapse.

Evidence for CHE in the low-Z environment of the SMC was presented by Martins et al. (2009) for SMC 1 and 2. The evidence for CHE was interpreted as being due to rapid stellar rotation. In the present study, line effects were not detected for these SMC objects and it would be unlikely that both of them are observed pole-on. It is therefore more likely that line-effect WR stars are special for reasons other than rotationally induced CHE. Vink et al. (2011) discovered a highly significant correlation between Galactic line-effect WR stars and WR stars with ejecta nebulae (see below).

Furthermore, another issue has come to light. In the original rotation-induced CHE models of Yoon & Langer (2005) GRB production was predicted to take place for initial masses as low as 20 $M_\odot$, but observations of GRB host galaxies prefer significantly higher initial masses, above 40 $M_\odot$ (Raskin et al. 2008; Levan et al. 2016), as GRBs are more concentrated on the brightest regions of their host galaxies than supernovae, hinting at more massive stars (Fruchter et al. 2006).

4.2. Alternative: post-luminous blue variables

For the Galactic sample, the high coincidence between line-effect WR stars and those WN stars with ejecta nebula suggested that the rotating WR subset are post-LBVs. Moreover, for the case of weak coupling between the stellar core and envelope, i.e. without the presence of a magnetic field (Hirschi et al. 2005; Petrovic et al. 2005; Georgy et al. 2013; Groh et al. 2013), the WR rotation rates inferred (see e.g. Chené & St-Louis 2010) are sufficiently large to fulfill the angular momentum conditions for GRB production (Vink et al. 2011; Gräfener et al. 2012). Whilst these Galactic line-effect WN stars (see bottom of Table 2) have the correct ingredients, they may not be GRB progenitors owing to their high metallicity.

In the current low-Z study, we found three line-effects in LMC WN stars. As was already noted, from the current study BAT99-70 is a WC star, whereas BAT99-43 is of WN type. The two line-effect stars from Vink (2007) are both very late-type WNL, WN9 objects. When considering the parameters of a very large sample of over 100 LMC WN stars of Hainich et al. (2014), the line-effect stars BAT99-22 and BAT99-33 do indeed stand out, as these late-type WN objects have far slower outflow velocities (only of order 400 km s^{-1}) than any of the other WR stars (with terminal wind velocities of thousands of km s^{-1}).

A potential reason for this could be that these winds are aspherical and observed close-to edge-on. Asphericity could be due to wind compression (Bjorkman & Cassinelli 1993; Ignace et al. 1996) or non-radial line forces (Owocki et al. 1996). However, 2D wind hydrodynamics calculations show that even for very rapid rotation one would only expect relatively small changes in the mass-loss rate, terminal wind velocity, and wind density as a function of latitude (Müller & Vink 2014). It is therefore more likely that the slow wind features in BAT99-22 and BAT99-33 are intrinsic to the type of star.

Interestingly, both BAT99-22 and BAT99-33 have in the past been classified as Ofpe/WN9 stars (Bohannan & Walborn 1989) and these objects are thought to be closely related to LBVs; this is the case especially since the Ofpe/WN9 star R 127 went into outburst (Stahl et al. 1983; Pasquali et al. 1997; Vink 2012).

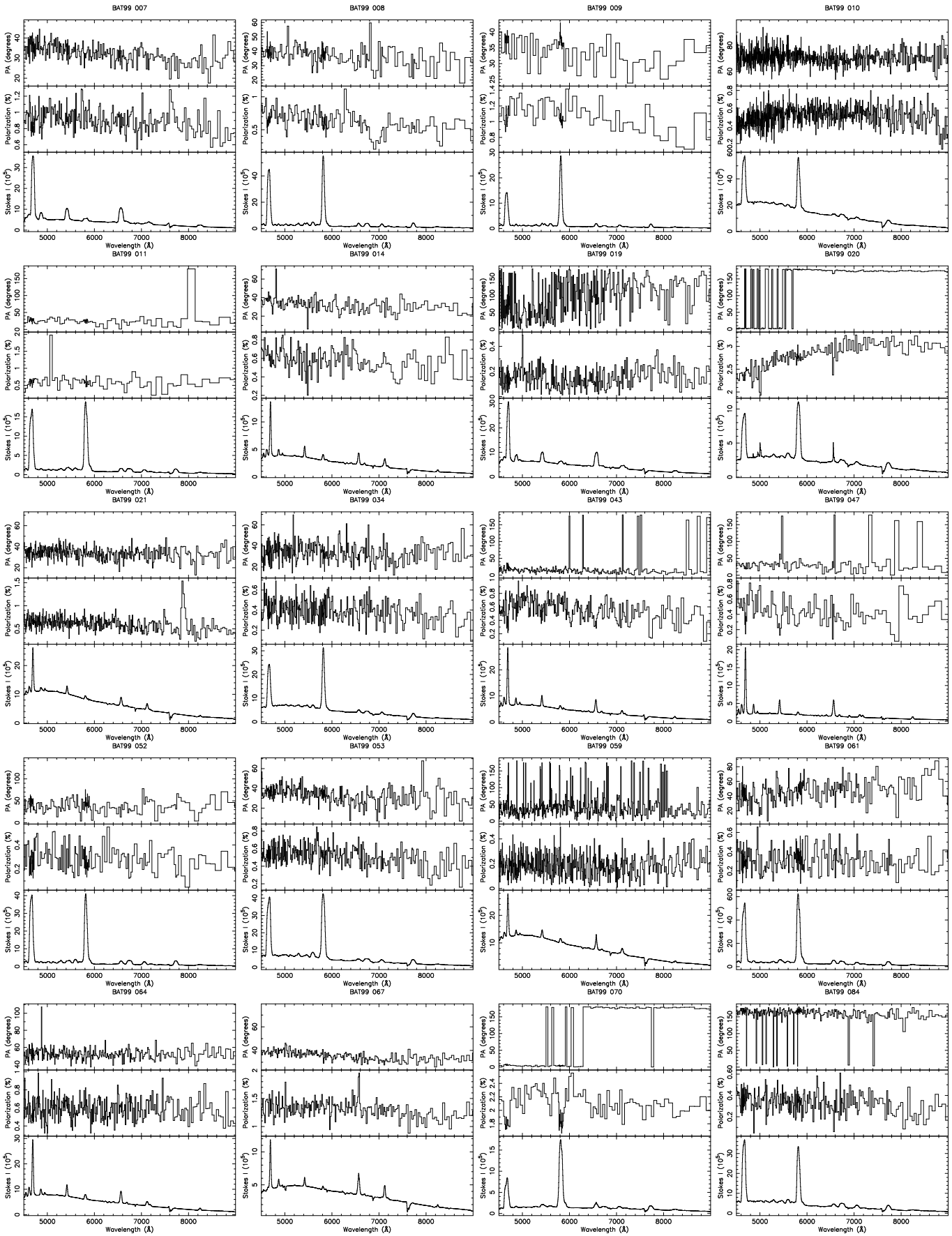

Fig. 3. Polarization spectra of LMC WR stars.

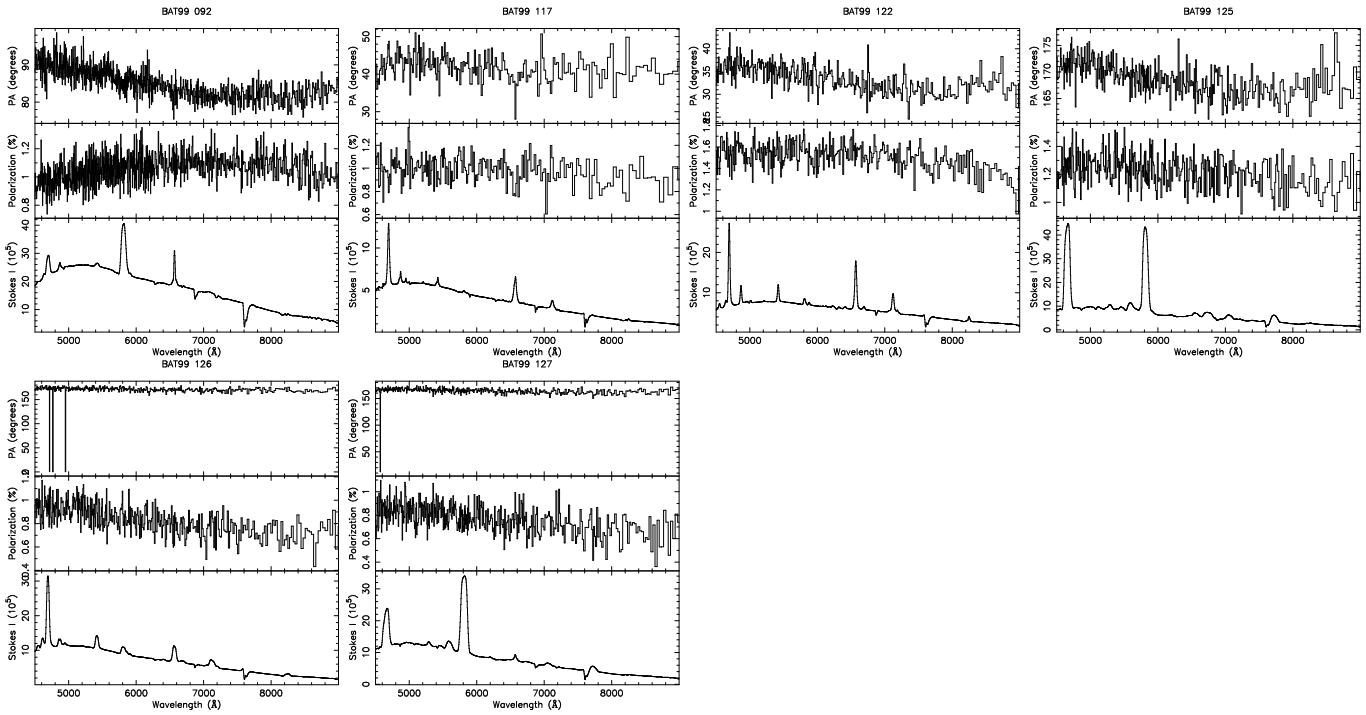

Fig. 4. Polarization spectra of the LMC WR objects continued.

Table 2. Stellar parameters for WN stars with a line effect.

WR	WR sub-type [kK]	$T_\star$	X_H	$\log L$ [$L_\odot$]	$R_\star$ [$R_\odot$]	$M_\star$ [$M_\odot$]	Γ_e	$\log(\dot{M})$ [$M_\odot$/yr]	v [km s^{-1}]
SMC									
HD 5980	WN5	45	0.25	6.35	24	88.4	0.48	–4.5	2200
						54.5	0.79		
LMC									
BAT99-22	WN9h	32	0.4	5.75	25.1	43.4	0.28	–4.85	400
						21.5	0.56		
BAT99-33	Ofpe/WN9	28	0.2	6.50	74.8	114.3	0.51	–4.43	400
						72.2	0.81		
BAT99-43	WN4o+OB	67	0.0	5.85	6.3	27.0	0.40	–5.15	1600
						24.8	0.44		
Milky Way									
6	WN4	89.1	0.0	5.6	2.65	17.9	0.342	–4.5	1700
16	WN8	44.7	0.25	6.15	19.9	40.1	0.678	–4.5	650
		41.7	0.23	5.68	12.3	20.0	0.453	–4.8	
40	WN8	44.7	0.23	6.05	17.7	34.3	0.618	–4.3	650
		45.0	0.15	5.61	10.6	18.2	0.397	–4.5	
134	WN6	63.1	0.0	5.6	5.29	17.9	0.342	–4.6	1700
136[3]	WN6	70.8	0.12	5.4	3.34	13.7	0.316	–4.7	1600

Notes. Parameters for the LMC WN stars are from Hainich et al. (2014), whilst the parameters for HD 5980 are from Shenar et al. (2016). The Galactic WN parameters are from Hamann et al. (2006). Masses $M_\star$ and Eddington factors Γ_e are obtained from the mass-luminosity relations for both homogeneously H-burning and He-burning by Gräfener et al. (2011). The spectroscopically determined mass-loss rates $\dot{M}$ are scaled to a wind clumping factor $D = 10$. See the discussion in Vink et al. (2011) on the inclusion of WR 136 as a line-effect object.

Furthermore, Nota et al. (1995) found that five of the Ofpe/WN9 stars show the presence of nebular emission lines, indicating a surrounding nebulosity.

There thus seems to be a coherent picture developing with respect to the LMC Ofpe/WN9 stars: they have slow outflow velocities, CS nebulae, and are predominately linearly polarized. One reason for the larger incidence of line effects amongst these later type WN stars could be that it is easier to detect asymmetries in a slower wind, as polarization levels seem to increase for larger stellar radii (Robert et al. 1989; Davies et al. 2005). However, this would not explain the correlation between line-effect WR stars and stars with ejecta nebula found by Vink et al. (2011). That correlation was interpreted as a link between rapid rotation and age. Young WR stars that have only recently

transitioned from the RSG or LBV phase may still maintain their rotation rates. From photometric periods Gräfener et al. (2012) estimated moderate rotation speeds of 36...120 km s^{-1} for line-effect WR stars. Assuming a fixed $\Omega = v_{\rm rot}/R_\star$ it is clear that the evolutionary progenitor radius cannot be much larger. For S Dor LBVs, such as AG Car and HR Car, $v_{\rm rot}$ is of order 200 km s^{-1} (Groh et al. 2009). With LBV radii of order 70 $R_\odot$, the associated late-type Galactic WN8 stars WR 16 and WR 40 with radii up to 20 $R_\odot$ are rather consistent with an LBV – WR evolutionary transition, whilst the large radii of Magellanic Cloud WR stars make the post-LBV scenario even more likely. Assuming a fixed Ω, a post-RSG scenario – with extremely large radii of $\gg$100 $R_\odot$ – would however require extremely rapidly rotating RSGs, which are not known.

Smith et al. (2004) noted that when post-RSG/LBV stars return from the red part of the HRD, where they may bounce several times against the cool side of the bi-stability jump[4], to the blue part of the HRD, on the hot side of the bi-stability jump, might appear as Ofpe/WN9 stars with slowly expanding ring nebulae. If the Ofpe/WN9 stars and line-effect objects may indeed be identified as post-RSG or post-LBV objects with a nebula, it is likely they would have lost a significant fraction of their mass, which brings them closer to their Eddington limit (Humphreys & Davidson 1994; Vink 2012). An object in close proximity to the Eddington limit would not only be subjected to a larger mass-loss rate (Castor et al. 1975; Vink & Gräfener 2012), but also a slower wind velocity (Castor et al. 1975; Gräfener & Hamann 2008), which might be the reason why Ofpe/WN9 stars such as BAT99-22 and BAT99-33 have such slow terminal velocities of just 400 km s^{-1}.

Can we link these WNL stars to the Galactic line-effect WN stars? Looking at the bottom of Table 2 it might be interesting to note that two of the five are the runaway WN8 stars, WR 16, and WR 40 (Walborn & Fitzpatrick 2000) with slow outflow speeds of order 650 km s^{-1}. For decades it has been known that Galactic WN8 stars are special (Moffat & Shara 1986; Crowther et al. 1995) in terms of their larger photometric variability, their association with ejecta nebulae, their low binary frequency, and relatively "isolated" spatial distribution. In this sense they share many of these properties with LBVs (see Smith & Tombleson 2015). Perhaps both their isolation (Kenyon & Gallagher 1985) and their low-binary frequency (Vink 2012) indicate a binary past.

In any case, taking the special properties of both LMC and Milky Way WNL stars together, the line-effect results indeed suggest a link between stellar rotation and the presence of a nebula. For LBVs, Gvaramadze & Kniazev (2017) suggested that isolated/runaway LBV stars are more likely to be surrounded by a CS nebula than for cluster-stars owing to the potential destructive effects of neighbouring massive stars, but this would not explain *why* isolated stars would rotate faster than clustered objects. It is therefore more likely there is a *physical* connection between stellar rotation and the presence of a nebula.

Next, we search for a possible link between the stellar rotation of GRB progenitors and the connection to wind/nebula features in afterglow spectra.

[4] The bi-stability jump is a strong mass-loss discontinuity at ~20 000 K (Petrov et al. 2016).

4.3. Circumstellar features in gamma-ray burst afterglow spectra

Absorption features in GRB afterglow spectra have been interpreted as either due to the absorption in the intervening interstellar medium (ISM) or the direct circumstellar medium (CSM). Interest was triggered by the case of GRB 021004 (Möller et al. 2002; Schaefer et al. 2003; Mirabal et al. 2003; Fiore et al. 2005; Starling et al. 2005; Castro-Tirado et al. 2010), which showed absorption features both at intermediate (~500 km s^{-1}) and high velocity (~3000–4000 km s^{-1}). Whilst the high velocity features could either be explained by the wind outflow speed of a classical WR star or acceleration by the radiation of the burst, the intermediate velocity of order ~500 km s^{-1} has been more challenging to explain.

Van Marle et al. (2005) performed hydrodynamical simulation of the evolution of the circumstellar medium around post-RSG/LBV stars that could potentially explain intermediate velocities, but WR nebula expansion speeds are far lower (Marston 1995) than predicted by van Marle et al. (2005).

If our post-LBV scenario for GRB progenitors that so nicely explains the correlation between stellar rotation and the presence of ejecta nebulae is correct, it might be relevant that the outflow speeds in both the LMC WN9/Ofpe and the Galactic WN8 stars are of order 500 km s^{-1}, which possibly accounts for intermediate velocities seen in GRB afterglow spectra.

Finally, although Chen et al. (2007) did not find any evidence for CS absorption features in the range −1000 to −5000 km s^{-1} within a sample of five GRBs, Fox et al. (2008) preferred a CS origin for at least some of their sample of seven.

4.4. The WR/LBV HD 5980: chemical homogeneous evolution after all?

Whilst the late-type WN LMC stars BAT-22 and BAT-33 might be explained by the post-LBV scenario, BAT-43 is earlier with a much smaller radius and a higher effective temperature (see Table 2). For this object some form of CHE might still be a more suitable scenario. Chemical homogeneous evolution might no longer be confined to low Z, as for instance Martins et al. (2013) suggested for cases at Galactic and LMC metallicity. Even for the very massive star (VMS) WN5h star VFTS 682, Bestenlehner et al. (2011) suggested that the high stellar effective temperature would be best explained by CHE. One should note that rapid rotation is not an absolute requirement for CHE, but it can also be caused by a large convective core and high mass-loss rates for VMS (Gräfener et al. 2011; Yusof et al. 2013; Vink 2015; Köhler et al. 2015).

The SMC binary system HD 5980 was suggested to be the result of CHE, making it a potential GRB progenitor (Koenigsberger et al. 2014). Our detection of a line effect in HD 5980 might thus be relevant. Given the challenges for rotation-induced CHE (Sect. 4.1), it seems more likely that CHE in HD 5980 is not due to rotation-induced CHE, but the result of VMS-specific physics of a large convective core and strong mass loss instead. We note that all line-effect WN stars in Table 2 have luminosities $\log(L/L_\odot) \geq 5.4$ (see Table 2), corresponding to initial masses above the required 40 $M_\odot$ for GRB production (Levan et al. 2016).

5. Summary

The detection of gravitational waves from a merging "heavy" black hole associated with GW 150914 has created a renewed

interest in the formation of stellar-mass black holes. One of the largest surprises was the very large mass of these objects, hinting at a low Z environment. In turn, lower Z may lead to less spin-down, and subsequently larger WR spin rates. The rotation rates of WR stars and black hole progenitors have thus become key aspects for our understanding of massive single and binary star evolution towards collapse. The most popular scenarios involve classical evolution through mass loss (e.g. Belczynski et al. 2016) and rapid rotation with quasi-CHE (e.g. de Mink & Mandel 2016; Marchant et al. 2016).

To obtain empirical constraints on black hole progenitor spin we measured wind asymmetries in all 12 known WR stars in the SMC at $Z = 1/5\ Z_\odot$, and also within a significantly enhanced sample of objects in the LMC at $Z = 1/2\ Z_\odot$, tripling the previous sample of Vink (2007). This total LMC sample size of 39 made it appropriate for comparison to the Galactic sample. We measured wind asymmetries with linear spectropolarimetry and we detected new line effects in the LMC WN star BAT99-43 and the WC star BAT99-70, as well as HD 5980 in the SMC, which we confirm to be evolving chemically homogeneously.

With previous reported line effects in the late-type WNL (Ofpe/WN9) objects BAT99-22 and BAT99-33, this brings the total LMC WR sample to four, i.e. a frequency of ~10%, which was not found to be higher than amongst the Galactic WR sample. As WR mass loss is likely Z-dependent, our Magellanic Cloud line-effect WR stars may maintain their surface rotation and fulfill the basic conditions for producing long GRBs.

The similar fraction of line-effect WR stars at low Z in comparison to the Milky Way casts doubt on the rotationally induced CHE scenario for producing GRBs and objects like GW 150914 (see Sect. 4.1). Instead, our data seem consistent with a post-LBV channel, or resulting from CHE due to physics specific to VMS, i.e. a large convective core and strong wind mass loss.

Acknowledgements. We would like to thank the anonymous referee for constructive comments. This research made use of the SIMBAD database, operated at CDS, Strasbourg, France. J.S.V. is funded by the Northern Ireland Department of Communities (DfC). T.J.H. was funded by ST/M0012174/1.

References

Abbott, B. P., Abbott, R., Abbott, T. D., et al. 2016, Phys. Rev. Lett., 116, 061102
Bartzakos, P., Moffat, A. F. J., & Niemela, V. S. 2001, MNRAS, 324, 18
Belczynski, K., Bulik, T., Fryer, C. L., et al. 2010, ApJ, 714, 1217
Belczynski, K., Holz, D. E., Bulik, T., & O'Shaughnessy, R. 2016, Nature, 534, 512
Bestenlehner, J. M., Vink, J. S., Gräfener, G., et al. 2011, A&A, 530, L14
Bjorkman, J. E., & Cassinelli, J. P. 1993, ApJ, 409, 429
Bohannan, B., & Walborn, N. R. 1989, PASP, 101, 520
Breysacher, J., Azzopardi, M., & Testor, G. 1999, A&AS, 137, 117
Brott, I., de Mink, S. E., Cantiello, M., et al. 2011, A&A, 530, A115
Cantiello, M., Yoon, S.-C., Langer, N., & Livio, M. 2007, A&A, 465, L29
Castor, J. I., Abbott, D. C., & Klein, R. I. 1975, ApJ, 195, 157
Castro-Tirado, A. J., Møller, P., García-Segura, G., et al. 2010, A&A, 517, A61
Chen, H.-W., Prochaska, J. X., Ramirez-Ruiz, E., et al. 2007, ApJ, 663, 420
Chené, A.-N., & St-Louis, N. 2010, ApJ, 716, 929
Crowther, P. A., Hillier, D. J., & Smith, L. J. 1995, A&A, 293, 403
Cucchiara, A., Levan, A. J., Fox, D. B., et al. 2011, ApJ, 736, 7
Davies, B., Oudmaijer, R. D., & Vink, J. S. 2005, A&A, 439, 1107
de Mink, S. E., & Mandel, I. 2016, MNRAS, 460, 3545
de Mink, S. E., Sana, H., Langer, N., Izzard, R. G., & Schneider, F. R. N. 2014, ApJ, 782, 7
Fiore, F., D'Elia, V., Lazzati, D., et al. 2005, ApJ, 624, 853
Foellmi, C., Moffat, A. F. J., & Guerrero, M. A. 2003, MNRAS, 338, 1025
Fox, A. J., Ledoux, C., Vreeswijk, P. M., Smette, A., & Jaunsen, A. O. 2008, A&A, 491, 189
Fruchter, A. S., Levan, A. J., Strolger, L., et al. 2006, Nature, 441, 463
Georgy, C., Ekström, S., Eggenberger, P., et al. 2013, A&A, 558, A103
Gräfener, G., & Hamann, W.-R. 2005, A&A, 432, 633
Gräfener, G., Vink, J. S., de Koter, A., & Langer, N. 2011, A&A, 535, A56
Gräfener, G., Vink, J. S., Harries, T. J., & Langer, N. 2012, A&A, 547, A83
Groh, J. H., Hillier, D. J., Damineli, A., et al. 2009, ApJ, 698, 1698
Groh, J. H., Georgy, C., & Ekström, S. 2013, A&A, 558, L1
Gvaramadze, V. V., & Kniazev, A. Y. 2017, ASP Conf. Ser., 508, 207
Hainich, R., Rühling, U., Todt, H., et al. 2014, A&A, 565, A27
Hainich, R., Pasemann, D., Todt, H., et al. 2015, A&A, 581, A21
Harries, T. J. 2000, MNRAS, 315, 722
Harries, T. J., & Howarth, I. D. 1996, A&A, 310, 533
Harries, T. J., Hillier, D., Howarth, I. D., et al. 1998, MNRAS, 296, 1072
Hayes, D. P. 1975, ApJ, 197, 55
Hirschi, R., Meynet, G., & Maeder, A. 2005, A&A, 443, 581
Hoffman, J. L., & Lomax, J. R. 2015, Wolf-Rayet Stars: Proc. Int. Workshop held in Potsdam (Germany: Universitätsverlag Potsdam)
Humphreys, R. M., & Davidson, K. 1994, PASP, 106, 1025
Ignace, R., Cassinelli, J. P., & Bjorkman, J. E. 1996, ApJ, 459, 671
Ignace, R., Hubrig, S., & Schöller, M. 2009, AJ, 137, 3339
Justham, S., Podsiadlowski, P., & Vink, J. S. 2014, ApJ, 796, 121
Kenyon, S. J., & Gallagher, J. S., III 1985, ApJ, 290, 542
Koenigsberger, G., Georgiev, L., Hillier, D. J., et al. 2010, AJ, 139, 2600
Koenigsberger, G., Morrell, N., Hillier, D. J., et al. 2014, AJ, 148, 62
Köhler, K., Langer, N., de Koter, A., et al. 2015, A&A, 573, A71
Levan, A., Crowther, P., de Grijs, R., et al. 2016, Space Sci. Rev., 202, 33
Lupie, O. L., & Nordsieck, K. H. 1987, AJ, 93, 214
Maeder, A., & Meynet, G. 2000, ARA&A, 38, 143
MacFadyen, A. I., & Woosley, S. E. 1999, ApJ, 524, 262
Marchant, P., Langer, N., Podsiadlowski, P., Tauris, T. M., & Moriya, T. J. 2016, A&A, 588, A50
Martins, F., Hillier, D. J., Bouret, J. C., et al. 2009, A&A, 495, 257
Martins, F., Depagne, E., Russeil, D., & Mahy, L. 2013, A&A, 554, A23
Marston, A. P. 1995, AJ, 109, 1839
Massey, P., & Duffy, A. S. 2001, ApJ, 550, 713
Massey, P., Olsen, K. A. G., & Parker, J. W. 2003, PASP, 115, 1265
Mathewson, D. S., & Ford, V. L. 1970, MmRAS, 74, 139
Mirabal, N., Halpern, J. P., Chornock, R., et al. 2003, ApJ, 595, 935
Moffat, A. F. J., & Shara, M. M. 1986, AJ, 92, 952
Møller, P., Fynbo, J. P. U., Hjorth, J., et al. 2002, A&A, 396, L21
Müller, P. E., & Vink, J. S. 2014, A&A, 564, A57
Nota, A., Livio, M., Clampin, M., & Schulte-Ladbeck, R. 1995, ApJ, 448, 788
Owocki, S. P., Cranmer, S. R., & Gayley, K. G. 1996, ApJ, 472, L115
Pasquali, A., Langer, N., Schmutz, W., et al. 1997, ApJ, 478, 340
Petrov, B., Vink, J. S., & Gräfener, G. 2016, MNRAS, 458, 1999
Petrovic, J., Langer, N., Yoon, S.-C., & Heger, A. 2005, A&A, 435, 247
Poeckert, R., & Marlborough, J. M. 1976, ApJ, 206, 182
Raskin, C., Scannapieco, E., Rhoads, J., & Della Valle, M. 2008, ApJ, 689, 358
Robert, C., Moffat, A. F. J., Bastien, P., Drissen, L., & St.-Louis, N. 1989, ApJ, 347, 1034
Sander, A., Hamann, W.-R., & Todt, H. 2012, A&A, 540, A144
Schaefer, B. E., Gerardy, C. L., Höflich, P., et al. 2003, ApJ, 588, 387
Shenar, T., Hainich, R., Todt, H., et al. 2016, A&A, 591, A22
Smith, N., & Tombleson, R. 2015, MNRAS, 447, 598
Smith, N., Vink, J. S., & de Koter, A. 2004, ApJ, 615, 475
Stahl, O., Wolf, B., Klare, G., et al. 1983, A&A, 127, 49
Starling, R. L. C., Wijers, R. A. M. J., Hughes, M. A., et al. 2005, MNRAS, 360, 305
St-Louis, N. 2013, ApJ, 777, 9
St-Louis, N., Drissen, L., Moffat, A. F. J., Bastien, P., & Tapia, S. 1987, ApJ, 322, 870
Tanvir, N. R., Fox, D. B., Levan, A. J., et al. 2009, Nature, 461, 1254
Tinbergen, J. 1996, in Astronomical Polarimetry, ed. Jaap Tinbergen (Cambridge, UK: Cambridge University Press), 174
van Marle, A. J., Langer, N., & García-Segura, G. 2005, A&A, 444, 837
Vink, J. S. 2007, A&A, 469, 707
Vink, J. S. 2012, Eta Carinae and the Supernova Impostors, 384, 221
Vink, J. S. 2015, Very Massive Stars in the Local Universe, Astrophys. Space Sci. Lib., 412
Vink, J. S., & de Koter, A. 2005, A&A, 442, 587
Vink, J. S., & Gräfener, G. 2012, ApJ, 751, L34
Vink, J. S., Drew, J. E., Harries, T. J., & Oudmaijer, R. D. 2002, MNRAS, 337, 356
Vink, J. S., Gräfener, G., & Harries, T. J. 2011, A&A, 536, L10
Walborn, N. R., & Fitzpatrick, E. L. 2000, PASP, 112, 50
Wolf, C., & Podsiadlowski, P. 2007, MNRAS, 375, 1049
Woosley, S. E., & Bloom, J. S. 2006, ARA&A, 44, 507
Woosley, S. E., & Heger, A. 2006, ApJ, 637, 914
Yoon, Y.-C., & Langer, N. 2005, A&A, 443, 643
Yusof, N., Hirschi, R., Meynet, G., et al. 2013, MNRAS, 433, 1114